

CHARACTERISATION AND *IN VITRO* AND *IN VIVO* EVALUATION OF SUPERCRITICAL-CO₂-FOAMED β -TCP/PLCL COMPOSITES FOR BONE APPLICATIONS

S. Pitkänen^{1,2*}, K. Paakinaho^{1,3,4}, H. Pihlman⁵, N. Ahola³, M. Hannula⁶, S. Asikainen⁷, M. Manninen⁴, M. Morelius⁵, P. Keränen⁵, J. Hyttinen⁶, M. Kellomäki³, O. Laitinen-Vapaavuori⁵ and S. Miettinen^{1,2}

¹Adult Stem Cell Group, BioMediTech, Faculty of Medicine and Health Technology, Tampere University, Tampere, Finland

²Research, Development and Innovation Centre, Tampere University Hospital, Tampere, Finland

³Biomaterials and Tissue Engineering Group, BioMediTech, Faculty of Medicine and Health Technology, Tampere University, Tampere, Finland

⁴Orton Orthopaedic Hospital, Helsinki, Finland

⁵Department of Equine and Small Animal Medicine, Faculty of Veterinary Medicine, University of Helsinki, Helsinki, Finland

⁶Computational Biophysics and Imaging Group, BioMediTech, Faculty of Medicine and Health Technology, Tampere University, Tampere, Finland

⁷Polymer Technology Research Group, Department of Chemical and Metallurgical Engineering, Aalto University, Espoo, Finland

Abstract

Most synthetic bone grafts are either hard and brittle ceramics or paste-like materials that differ in applicability from the gold standard autologous bone graft, which restricts their widespread use. Therefore, the aim of the study was to develop an elastic, highly porous and biodegradable β -tricalciumphosphate/poly(L-lactide-co- ϵ -caprolactone) (β -TCP/PLCL) composite for bone applications using supercritical CO₂ foaming. Ability to support osteogenic differentiation was tested in human adipose stem cell (hASC) culture for 21 d. Biocompatibility was evaluated for 24 weeks in a rabbit femur-defect model. Foamed composites had a high ceramic content (50 wt%) and porosity (65-67 %). After 50 % compression, in an aqueous environment at 37 °C, tested samples returned to 95 % of their original height. Hydrolytic degradation of β -TCP/PLCL composite, during the 24-week follow-up, was very similar to that of porous PLCL scaffold both *in vitro* and *in vivo*. Osteogenic differentiation of hASCs was demonstrated by alkaline phosphatase activity analysis, alizarin red staining, soluble collagen analysis, immunocytochemical staining and qRT-PCR. *In vitro*, hASCs formed a pronounced mineralised collagen matrix. A rabbit femur defect model confirmed biocompatibility of the composite. According to histological Masson-Goldner's trichrome staining and micro-computed tomography, β -TCP/PLCL composite did not elicit infection, formation of fibrous capsule or cysts. Finally, native bone tissue at 4 weeks was already able to grow on and in the β -TCP/PLCL composite. The elastic and highly porous β -TCP/PLCL composite is a promising bone substitute because it is osteoconductive and easy-to-use and mould intraoperatively.

Keywords: Bone substitute, composite, adipose stem cells, osteogenic differentiation, rabbit distal femur defect, β -tricalciumphosphate, poly(L-lactide-co- ϵ -caprolactone).

***Address for correspondence:** Sanna Pitkänen, BioMediTech, Faculty of Medicine and Health Technology, FI-33014 Tampere University, Tampere, Finland.

Telephone number: +358 401901789 Email: sanna.pitkanen@tuni.fi

Copyright policy: This article is distributed in accordance with Creative Commons Attribution Licence (<http://creativecommons.org/licenses/by-sa/4.0/>).

Introduction

Bone is the second most commonly transplanted tissue, with approximately 2.2 million orthopaedic

surgeries carried out worldwide annually (Campana *et al.*, 2014; Kinaci *et al.*, 2014; Van der Stok *et al.*, 2011). As people age, this number is expected to rise. Among bone transplants, autologous bone is considered

the gold standard, while allogenic bone and bone substitutes are also used. Important patient groups affected by problems concerning bone transplants are young children, who do not have enough bone tissue to be harvested, and elderly people, whose bone quality is weak. In addition, several problems are related to the use of autologous bone transplants, such as morbidity of the harvesting site, insufficiency and viability of the harvested bone and infection (Freeman and McNamara, 2017; Van der Stok *et al.*, 2011). Furthermore, even though allograft bone may provide enough bone, transplanted tissue might be rejected; also, proteins and osteoinductive factors might be denaturated following sterilisation (Boyce *et al.*, 1999). Moreover, when using allografts, disease transmission and infection are recurring problems, as 18 % of donated femoral heads have been shown to be affected by bacterial or fungal infections (Barbour and King, 2003; Boyce *et al.*, 1999; Freeman and McNamara, 2017). Therefore, there is an evident and growing need for safe, synthetic bone transplants and tissue engineering strategies.

Even though various biomaterials have been proposed for bone replacement, the study and development of these structures have rarely proceeded to clinical applications (de Misquita *et al.*, 2016). Before a bone substitute can become a clinically used product, its efficacy and safety has to be demonstrated both *in vitro* and *in vivo* as well as in a clinical trial. According to the regulation (EU) 2017/745 of the European Parliament and of the Council of 5 April 2017 on medical devices, a product cannot receive a CE mark without clinically proven data (Web ref. 1). An ideal bone substitute should be osteoconductive or osteoinductive, biocompatible, biodegradable (Van der Stok *et al.*, 2011) and highly porous, with a pore size larger than 250 μm to allow cell and tissue ingrowth (Mathieu *et al.*, 2005; Turnbull *et al.*, 2017; Zadpoor, 2015) and vascularisation (Rouwkema *et al.*, 2008). Furthermore, the implant should not induce the formation of fibrotic tissue (Van der Stok *et al.*, 2011) or infection. Cost-effective, large-scale manufacturing is also important when designing a new bone substitute for clinical use.

Ceramics, such as hydroxyapatite and other calcium phosphates, are highly compatible with bone tissue and, therefore, the most widely used synthetic bone substitute materials for treating large bone defects. Among calcium phosphates, β -tricalciumphosphate (β -TCP) induces significantly more bone in an ectopic site *in vivo* as compared to hydroxyapatite (Chatterjea *et al.*, 2013; Yuan *et al.*, 2010) and, therefore, β -TCP was chosen as the calcium phosphate phase of the composite. However, there has been conflicting results concerning the osteoinductive properties of β -TCP and speculation that they might vary according to the surface properties of the material (Bohner and Miron, 2019; Duan *et al.*, 2018). Calcium phosphate materials are hard and brittle, making them difficult to shape intraoperatively and implant. Synthetic

polymers such as polylactide, polyglycolide, poly- ϵ -caprolactone and their copolymers are biocompatible and support osteogenic differentiation of stem cells *in vitro* (Campana *et al.*, 2014; Jeong *et al.*, 2008; Temple *et al.*, 2014; Wang *et al.*, 2016). Poly(L-lactide-co- ϵ -caprolactone) (PLCL) is a copolymer of L-lactide and ϵ -caprolactone with highly desirable characteristics as an implant material: elasticity, flexibility, high tensile strength, controllable degradation rate and good biocompatibility (Holmbom *et al.*, 2005; Wang *et al.*, 2016). PLCL scaffolds have been used in bone tissue engineering although, as PLCL is inert, hydrophobic and lacks biological recognition sites, the interaction with tissue and cells is not good enough either *in vitro* or *in vivo* (Jeong *et al.*, 2008; Wang *et al.*, 2016). By using supercritical CO₂ (scCO₂) processing, it was possible to create a homogenous, porous composite of the bioactive β -TCP and elastic PLCL. scCO₂ foaming was chosen as the processing technique as it is easy, cost-effective and non-toxic. Furthermore, the technique enables the production of polymeric structures with different pore sizes and total porosities. Briefly, CO₂ becomes a supercritical fluid above its critical temperature and pressure (31.10 °C, 73.9 bar), adapting characteristics between a liquid and a gas. Polymeric materials can be dissolved in scCO₂ and, as the pressure is decreased controllably, the CO₂ gas nucleation and expansion creates the wanted porous structure inside the polymeric material (Mathieu *et al.*, 2005).

Multipotent human adipose stem cells (hASCs) are easily available. Furthermore, hASCs have been widely studied in the field of bone tissue engineering *in vitro* (Kyllönen *et al.*, 2013a; Kyllönen *et al.*, 2013b; Ojansivu *et al.*, 2015; Tirkkonen *et al.*, 2013; Vanhatupa *et al.*, 2015) and *in vivo* (Jeon *et al.*, 2008; Wilson *et al.*, 2012). Therefore, hASCs are a relevant cell type for studying both the cytocompatibility of a potential bone substitute and the ability of a scaffold to support osteogenic differentiation *in vitro*.

The aim of the current study was to overcome the major limitations of previous bone-application-intended materials, to develop an elastic, highly porous, biodegradable and biocompatible β -TCP/PLCL composite for bone applications by using scCO₂ and to test its performance both *in vitro* and *in vivo*. Furthermore, the aim was to create a composite mimicking the mechanical properties of cartilaginous soft callus, which serves as the natural scaffold for bone regeneration during bone healing. For the first time, it was shown that scCO₂ processing of β -TCP/PLCL composite with a high ceramic content (50 wt%) could be used to produce scaffolds with porosity as high as 65-67 %. Furthermore, β -TCP granules were brought to the surface of the composites by a dynamic compression treatment. *In vitro* studies with hASCs demonstrated both cytocompatibility and osteogenic capacity of the scaffold. Furthermore, biocompatibility, osteoconductivity and bone tissue ingrowth were shown *in vivo* in a rabbit femur defect model.

Materials and Methods

Composite manufacturing and characterisation

Composites were manufactured by melt-mixing PLCL-polymer (70L/30CL; Purasorb PLC7015, Corbion Purac Biomaterials, Gorinchem, the Netherlands) with 50 wt% β -TCP, having a particle size range between 100 and 300 μ m (Plasma Biotol Ltd., Buxton, UK). Composites were foamed using scCO₂, as described in the granted patent (Web ref. 2), by using a Supercritical Carbon Dioxide Reactor System (SFE250, Waters Ltd., MA, USA). The residual lactide monomer content was measured by gas chromatography (DC8000, CE Instruments, Rodano, Italy) after post-melting. Foamed blocks were cut into discs for *in vitro* studies [diameter (\varnothing) = 8 mm, height (h) = 3 mm] and into cylinders for *in vivo* studies for cancellous bone (\varnothing = 3.2 mm, h = 10 mm) and intramuscular implantation (\varnothing = 4.0 mm, h = 10 mm). All samples were sterilised by γ -irradiation with a minimum dose of 25 kGy.

Prior to *in vitro* and *in vivo* studies, elastic scaffolds were treated by dynamically pre-compressing them repeatedly in an aqueous environment at 37 °C for a minimum of 20 cycles and compression level of at least 50 %. Composites were imaged by using a scanning electron microscope (SEM; Philips XL-30) and Xradia MicroXCT-400 X-ray imaging system with a voxel size of 5.6 μ m (Carl Zeiss X-ray Microscopy Inc.) before and after the compression treatment. Porosities and pore sizes were calculated from micro-computed tomography (μ CT) images with Fiji (Schindelin *et al.*, 2012) using BoneJ (Doube *et al.*, 2010) plugin. All the visualisations were conducted with Avizo 9.3.0 Software (Thermo Fisher Scientific).

Mechanical testing of composites

Mechanical testing was performed for both intact and pre-compressed samples (\varnothing = 8 mm, h = 3.5 \pm 0.6 mm), as dry at room temperature (RT) and in an aqueous environment at 37 °C using the Instron Electropuls E1000 (High Wycombe, UK) by compressing unconfined samples 1 mm/min until a 50 % strain was reached. Used crosshead speed was adapted from the standard ISO 604. Elastic modulus was determined from linear section of the stress-strain curve, between 0 and 20 % strain.

Hydrolytic degradation of composites *in vitro* and *in vivo*

Hydrolytic degradation of the porous composites *in vitro* was studied at 4, 12 and 24 weeks at 37 °C in Sørensen buffer solution (n = 6) and *in vivo* as intramuscular implantation on underside of the supraspinatus muscle (n = 6 at 4 and 12 weeks; n = 1 at 24 weeks due to strong scaffold degradation). A porous PLCL (70/30) polymer scaffold was used as a reference. Degradation was monitored by size exclusion chromatography (SEC) utilising a Waters Associates system equipped with a Waters 717Plus Satellite autosampler, a Waters 510 HPLC solvent

pump, two linear PL gel 5 μ m columns connected in series and a Waters 2414 differential refractometer. The number-average molecular weight (M_n), weight-average molecular weight (M_w) and polydispersity of the samples were determined against polystyrene standards at RT. Chloroform was used as the eluent and was delivered at a flow rate of 1 mL/min. Samples were dissolved in chloroform at a polymer concentration of 13.5 ppm. The injection volume was 100 μ L.

Isolation, characterisation and seeding of hASCs *in vitro*

hASCs were isolated from adipose tissue samples obtained from three female donors (40 \pm 11 years old) undergoing surgical procedures at the Department of Plastic Surgery, Tampere University Hospital after patients gave their consent. The study was conducted in accordance with the Ethics Committee of the Pirkanmaa Hospital District, Tampere (R15161).

Isolation of hASCs was conducted using a mechanical and enzymatic protocol as described previously (Lindroos *et al.*, 2009). Isolated hASCs were expanded in basic medium (BM) consisting of Dulbecco's modified Eagle's medium: nutrient mixture F-12 (DMEM/F-12 1 : 1; Thermo Fischer Scientific), 5 % human serum (HS; BioWest, Nuaille, France), 1 % antibiotics (100 U/mL penicillin; 100 U/mL streptomycin; Lonza) and 1 % L-glutamine (GlutaMAX I; Thermo Fischer Scientific). hASCs were cultured at 37 °C in 5 % CO₂ and medium was changed twice a week. Cells were detached with TrypLE Select (Life Technologies). Experiments were carried out at passage 3.

To verify the mesenchymal origin of the cells, surface marker expression of hASCs at passage 1 was characterised by fluorescent-activated cell sorter (FACSaria; BD Biosciences) as described previously (Lindroos *et al.*, 2009). Monoclonal antibodies against CD14-PE-Cy7, CD19-PE-Cy7, CD45RO-APC, CD73-PE, CD90-APC (BD Biosciences), CD34-APC, HLA-DR-PE (Immunotools, Friesoythe, Germany) and CD105-PE (R&D Systems) were used. The analysis was performed on 10,000 cells per sample and unstained hASC samples were used to compensate for the background autofluorescence levels. The expression of the surface markers CD73, CD90 and CD105 was positive, the expression of CD14, CD19, CD45 and human leukocyte antigen DR isotype (HLA-DR) was negative and that of CD34 was moderate (Table 1). The surface markers' expression of hASCs confirmed the mesenchymal origin of the cells (Dominici *et al.*, 2006).

Before cell seeding, sterile composites were pre-compressed in BM and incubated for 24 h in BM at 37 °C. hASCs were seeded in a 50 μ L medium drop at a density of 510 cells/mm³ into the scaffolds. Cells were allowed to attach for 2-3 h before 500 μ L of BM or osteogenic medium (OM) were added. OM consisted of BM with the addition of 250 μ M ascorbic acid 2-phosphate (Sigma-Aldrich), 10 mM

Table 1. Surface marker expression of hASCs at passage 1. Positive > 98 %; negative < 2 %; moderate < 50 % > 2 %. SD: standard deviation.

Surface marker		mean \pm SD	expression
CD14	Serum lipopolysaccharide binding protein	0.6 \pm 0.6	negative
CD19	B lymphocyte-lineage differentiation antigen	0.4 \pm 0.2	negative
CD34	Sialomucin-like adhesion molecule	34.8 \pm 32.2	moderate
CD45	Leukocyte common antigen	1.6 \pm 0.3	negative
CD73	Ecto-50-nucleotidase	98.2 \pm 1.3	positive
CD90	Thy-1 (T-cell surface glycoprotein)	99.8 \pm 0.1	positive
CD105	SH-2, endoglin	98.3 \pm 1.2	positive
HLA-DR	Major histocompatibility class II antigens	0.6 \pm 0.1	negative

β -glycerophosphate (Sigma-Aldrich) and 5 nM dexamethasone (Sigma-Aldrich). As a 2-dimensional (2D) control for alizarin red staining, 500 cells were seeded in 1 mL of BM or OM in a 24-well plate (Nunc, Roskilde, Denmark).

Cell viability and proliferation

Cell viability was evaluated qualitatively by staining hASCs with fluorescent live/dead-staining probes (Molecular Probes) after 7, 14 and 21 d. hASCs were incubated for 45 min at RT with a mixture of 0.5 μ M calcein acetoxymethyl ester (Molecular Probes) and 0.25 μ M ethidium homodimer-1 (Molecular Probes). Images of living cells (green fluorescence) and dead cells (red fluorescence) were acquired using an Olympus IX51 phase contrast microscope with fluorescence optics and Olympus DP30BW camera (Olympus).

Cell number was analysed quantitatively after at 7, 14 and 21 d by analysing the total amount of DNA by CyQUANT Cell Proliferation Assay Kit (Molecular Probes), according to manufacturer's protocol, as reported previously (Kyllönen *et al.*, 2013a). Samples were analysed after two freeze-thaw cycles and fluorescence was measured at 480/520 nm with a microplate reader (Victor 1420 Multilabel Counter; Wallac, Turku, Finland).

Analysis of osteogenic differentiation *in vitro*

Alkaline phosphatase (ALP) activity was determined after 7, 14 and 21 d, as described previously (Kyllönen *et al.*, 2013a). ALP activity was determined from the same cell lysates as total DNA content. Absorbance was measured at 405 nm (Victor 1420).

Soluble total collagen was analysed at 7, 14 and 21 d by Soluble Collagen Assay Sircol™ (Biocolor, Carrickfergus, UK), as described previously (Tirkkonen *et al.*, 2013). Briefly, collagen was dissolved for 2 h at 4 °C with 0.5 M acetic acid (Merck) containing 0.1 mg/mL pepsin (Sigma-Aldrich), while gently shaking. Thereafter, 100 μ L samples were dyed with 500 μ L of Sircol™ Dye Reagent (Sirius red in picric acid; Biocolor) for 30 min at RT, while gently

shaking. Then, samples were centrifuged for 10 min at 13,400 \times g and the dyed collagen pellets were washed with 750 μ L of ice-cold Acid-Salt Wash Reagent (Biocolor). After another 10 min centrifugation at 13,400 \times g, the dye was diluted by adding 250 μ L of Alkali Reagent (Biocolor) on top of the dyed collagen pellet. Intensity of the dye was measured from two parallel 100 μ L samples in a 96-well plate (Nunc) using a microplate reader (Victor 1420).

Mineralisation was studied by alizarin red S staining after 14 and 21 d, as described previously (Kyllönen *et al.*, 2013a). In brief, paraformaldehyde (Sigma-Aldrich)-fixed cell-scaffold constructs were stained with filtered 2 % alizarin red S (pH 4.2; Sigma-Aldrich) and photographed after several washing steps. Dye was extracted with cetylpyridinium chloride (100 mM, Sigma-Aldrich) and its intensity was determined by measuring the absorbance at 540 nm (Victor 1420).

Quantitative real-time reverse transcription polymerase chain reaction (qRT-PCR) analysis was used to compare the relative expression of osteogenic genes in different experimental groups. Total RNA was isolated from hASCs at 14 and 21 d using the NucleoSpin RNA II kit reagent (Macherey-Nagel) according to the manufacturer's protocol. Single-strand cDNA was synthesised from total RNA using the High-Capacity cDNA Reverse Transcriptase Kit (Applied Biosystems). Data were normalised to the expression of the housekeeping gene human acidic ribosomal phosphoprotein large P0 (*hRPLP0*). Primer sequences and accession numbers for *RPLP0* and osteogenic genes *RUNX2a*, *OSTERIX* and *DLX5* are listed in Table 2. The qRT-PCR mixture contained cDNA, primers and SYBR Green PCR Master Mix (Applied Biosystems). Reactions were conducted with ABI PRISM® 7300 Sequence Detection System as reported previously (Kyllönen *et al.*, 2013a). Results were processed with ABI PRISM® 7300 Sequence Detection System-software (Applied Biosystems).

Osteogenic marker proteins collagen type I (COL-I) and osteocalcin (OCN) were detected with an indirect immunocytochemical staining method. At 7, 14 and

Table 2. Primer sequences and accession numbers of genes analysed by qRT-PCR.

Name	Full name	Accession number		Sequence	Product size (bp)
hRPLP0	Ribosomal protein, large, P0	NM_001002	Forward	5'-AAT CTC CAG GGG CAC CAT T-3'	70
			Reverse	5'-CGC TGG CTC CCA CTT TGT-3'	
hALP	Alkaline phosphatase	NM_000478.4	Forward	5'-CCC CCG TGG CAA CTC TAT CT-3'	73
			Reverse	5'-GAT GGC AGT GAA GGG CTT CTT-3'	
hRUNX2A	Runx2A, variant 1	NM_001024630.3	Forward	5'-CTT CAT TCG CCT CAC AAA CAA C-3'	62
			Reverse	5'-TCC TCC TGG AGA AAG TTT GCA-3'	
hOSX	Osterix	AF_477981	Forward	5'-TGA GCT GGA GCG TCA TGT G-3'	79
			Reverse	5'-TCG GGT AAA GCG CTT GGA-3'	
hDLX5	Distal-less homeobox 5	NM_005221.5	Forward	5'-ACC ATC CGT CTC AGG AAT CG-3'	75
			Reverse	5'-CCC CCG TAG GGC TGT AGT AGT-3'	

21 d, hASCs were fixed with 4 % paraformaldehyde (Sigma Aldrich) in Dulbecco's phosphate-buffered saline (DPBS) with 0.05 % Triton-X 100 (Sigma Aldrich) for 10 min followed by washing steps. Cells were blocked in 1 % bovine serum albumin (BSA) in DPBS for 1 h at 4 °C. Primary antibodies mouse monoclonal anti-COL-I (dilution 1 : 2,000; Abcam) and mouse monoclonal anti-OCN (dilution 1 : 100; Abcam) were diluted in 1 % BSA and incubated overnight at 4 °C. As a negative control, 1 % BSA without primary antibody was used. After washing steps, secondary antibody donkey anti-mouse AlexaFluor 488 IgG (dilution 1 : 1,000; Invitrogen) diluted in 1 % BSA was added and incubated for 45 min at RT. Cells were washed repeatedly and treated with 0.1 % 4,6-diamidino-2-phenylindole (DAPI) (Sigma Aldrich) in DPBS for 5 min at RT. Finally, cells were washed and imaged using an Olympus IX51 phase contrast microscope with fluorescence optics and Olympus DP30BW camera (Olympus). Images were edited with Adobe Photoshop version CS4.

Animal experiments

The Finnish Animal Experiment Board (ESAVI/5398/04.10.07/2014) approved the animal study and used protocols. 20 female New Zealand white rabbits were used.

Anaesthesia was induced by subcutaneous injection of ketamine (35 mg/kg, Ketador vet[®] 100 mg/mL, Richter Pharma, Wels, Austria) and medetomidine (0.3 mg/kg, Domitor[®] 1 mg/mL, OrionPharma, Espoo, Finland). Intravenous propofol boluses (2-5 mg/rabbit, Vetofol[®] 10 mg/mL, Norbrook Laboratories, Newry, Ireland), ketamine bolus (10 mg/kg) or mask anaesthesia with 1.5 % isoflurane (IsoFlo[®] vet 100%, Abbott Laboratories, Chicago, IL, USA) were used during the surgical procedure if needed. Intravenous trimethoprim/sulfamethoxazole (15 mg/kg, Duoprim[®] 200/40 mg/mL, Intervet International, Boxmeer, the Netherlands) was used as an antibiotic prophylaxis. Intravenous carprophen (4 mg/kg, Norocarp[®] 50 mg/mL, Norbrook Laboratories) and

buprenorphine (0.03 mg/kg, Bupaq[®] 0.3 mg/mL, Richter Pharma) were used as a pain medication.

A 20 mm skin incision was made on the lateral aspect of the right femoral condyle and a 3.2 mm diameter and 10 mm deep drilling hole was made above the lateral collateral ligament. Composites were moistened and pre-compressed in blood collected from the drilling hole prior to implantation. The drilling hole was filled with 3.2 × 10 mm cylinder-shaped β -TCP/PLCL composite implant and periosteum and skin were closed.

For the degradation study, a skin incision was made midline over the spine between the scapulae and two 4 × 10 mm β -TCP/PLCL composites were inserted through an applicator tube to the right supraspinatus muscle and two 4 × 10 mm polymer implants to the left supraspinatus muscle. Subcutaneous atipametzole (0.75 mg/kg, Antisedan[®] 5 mg/mL, OrionPharma) was used to reverse the sedative effect of the medetomidine after the procedure. For postoperative pain, subcutaneous buprenorphine (0.03 mg/kg) and carprophen (4 mg/kg) were used. Subcutaneous metoclopramide (0.2 mg/kg, Primperan[®] 5 mg/mL, Sanofi Oy, Espoo, Finland) was used to increase the intestinal motility. Rabbits were in a cage rest for 2 weeks after the surgery and, then, in a large-group housing area. They had access to hay and water *ad libitum*. One rabbit died during the procedure due to anaesthesia-related causes and one died 3 d after the operation as a result of a complication unrelated to the femoral defect.

The 18 rabbits were randomly divided in groups of 6 animals and euthanised 4, 12 and 24 weeks after the procedure. Subcutaneous injection of medetomidine (0.3 mg/kg) and ketamine (35 mg/kg) was followed by intracardial injection of pentobarbital (300 mg/rabbit, Mebunat[®] vet 60 mg/mL, Orion Pharma Oy, Espoo, Finland). The intramuscular implants were collected for further analysis.

μ CT analysis (MicroXCT-400, Zeiss) was performed on all the harvested femoral condyles

before histological preparation. Tube voltage of 120 kV and tube current of 83 μ A were selected. From each sample, 1,600 projections were taken with a 13.4 μ m voxel size. Exposure time was 4 s. Projections were reconstructed with the manufacturer's XMReconstructor software. Image processing and analysis were done with Avizo Software (Thermo Fisher Scientific). Thereafter, the femoral condyles were fixed in 10 % buffered formalin solution

followed by routine ascending ethanol series and methyl methacrylate embedding. A hard-tissue microtome (Leica, SM2500) was used to cut 5 μ m-thick slice. Masson-Goldner's Trichrome (MGT) staining was performed.

Statistical analysis

Statistical analysis was performed with SPSS version 23 (IBM) using a non-parametric test, due to the small

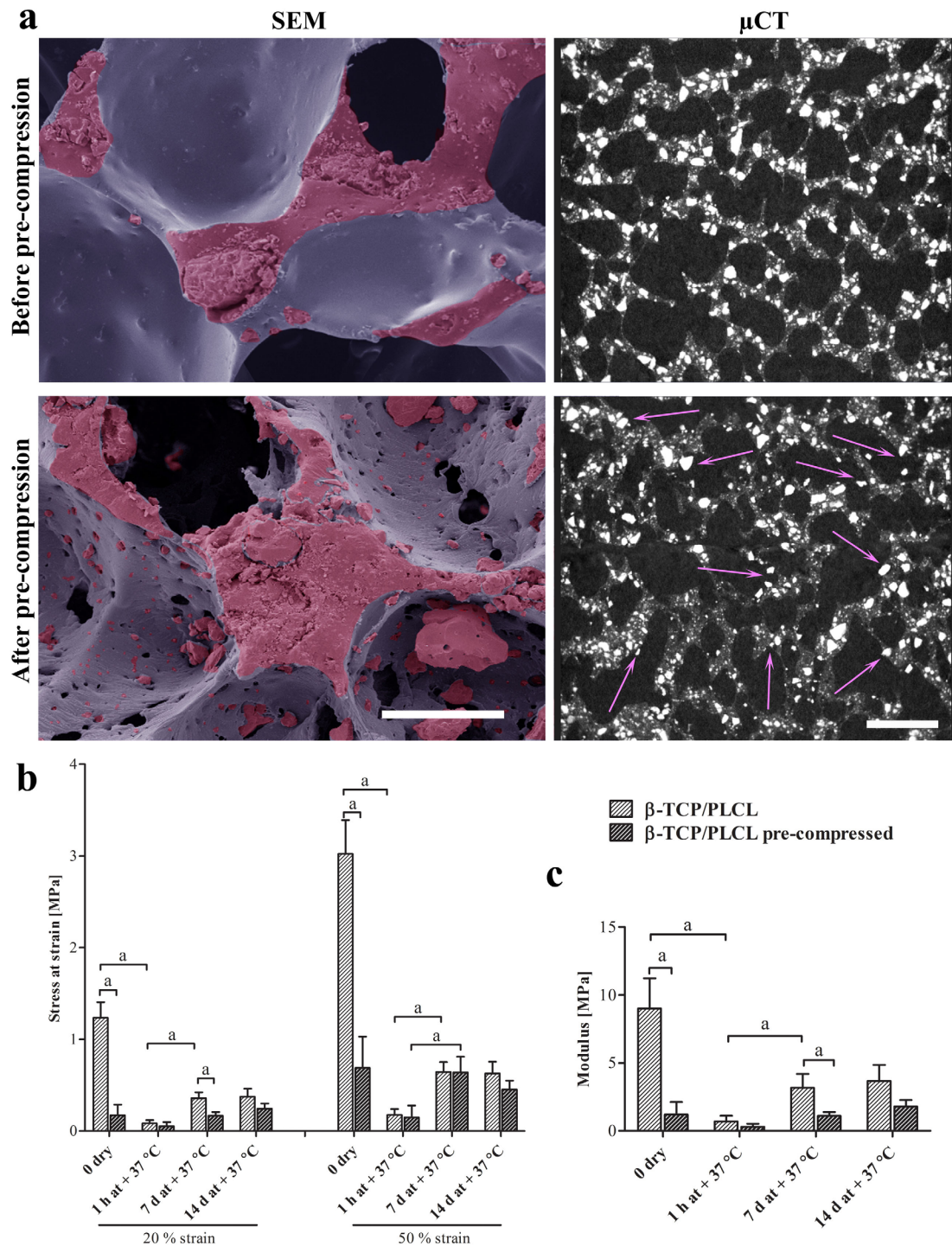


Fig. 1. β -TCP/PLCL composite characteristics before and after pre-compression treatment. (a) Representative SEM (scale bar: 200 μ m; PLCL coloured violet; β -TCP coloured pink) and μ CT (arrows indicate the granules released from under the polymer film; scale bar: 1,000 μ m) images. (b) Compressive stress at 20 and 50 % strain when dry and 1 h, 7 or 14 d at 37 °C in aqueous environment. (c) Modulus when dry and 1 h, 7 or 14 d at 37 °C in aqueous environment. Statistical significances indicated as ^a $p \leq 0.05$ ($n = 6$).

sample size. The effects of stress and strain ($n = 6$) on intact and pre-compressed composites and of pre-compressing and incubation at 37 °C on modulus ($n = 6$) of composites were compared using Mann-Whitney U-test with Bonferroni correction. Effects of BM or OM in combination with the composite on cell number, ALP activity, mineralisation, soluble collagen amount and gene expression were compared using Mann-Whitney U-test with Bonferroni correction. Results were considered significant when $p < 0.05$. Experiments for cell number, ALP activity, mineralisation and soluble collagen amount were repeated with 3 donor lines each with 3 parallel samples ($n = 9$). Experiments for gene expression were repeated with 3 donor lines each with 2 parallel samples ($n = 6$).

Results

Characteristics of the composite

Scaffold porosity was 65-67 %, with an average pore size of $380 \pm 130 \mu\text{m}$. In addition, compressive stress at 20 and 50 % strain and modulus were analysed at different time points. SEM images (Fig. 1a) showed that before pre-compression treatment, β -TCP (coloured pink) was mainly on the cutting surface of the composite, while the surfaces of the pores were smooth and a PLCL film (coloured violet) mainly covered the β -TCP granules. However, the effect of the pre-compression was evident, as after the protocol

the PLCL surface of the pores had ruptured and β -TCP granules protruded through it. Furthermore, SEM images demonstrated that the treatment tore additional holes in the pores of the composite. μCT images agreed with SEM images as they revealed that after the treatment more β -TCP granules were on display on the pore surfaces or even detached from the polymer phase in contrast to intact composite (Fig. 1a).

Both the compression treatment and warming at 37 °C had a significant effect on the mechanical properties of the composite. The compression treatment of a dry composite decreased the modulus significantly in contrast to an intact composite, but 1 h at 37 °C aqueous solution treatment erased such a difference (Fig. 1c). The same phenomenon was seen in the compressive stress analysis at both 20 and 50 % strain (Fig. 1b). Moreover, warming and wetting of the intact composite significantly decreased the modulus in comparison to dry intact composite (Fig. 1c). Intriguingly, both modulus and strength increased between 1 h and 7 d in an aqueous environment at 37 °C (Fig. 1b,c). No samples were broken during the compression analysis and samples tested in an aqueous environment at 37 °C returned to 95 % of their original height after the 50 % compression.

Hydrolytic degradation of the composite *in vitro* and *in vivo*

Molecular weight (M_n and M_w) change, caused by hydrolytic degradation of the polymer chains in

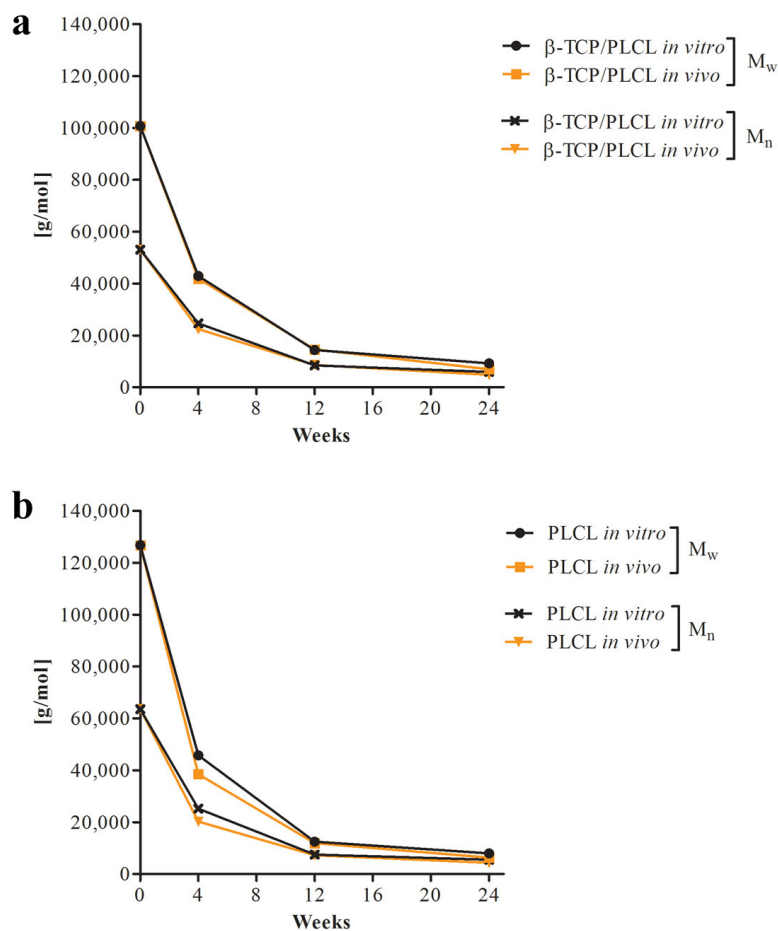


Fig. 2. Hydrolytic degradation analysis results. M_n and M_w of (a) β -TCP/PLCL composites and (b) PLCL scaffolds were analysed *in vitro* and *in vivo* after 4, 12 and 24 weeks.

both β-TCP/PLCL composites (Fig. 2a) and PLCL polymer scaffolds (Fig. 2b), was analysed both *in vitro* and *in vivo*. M_n and M_w of the samples were determined at 4, 12 and 24 weeks and the results showed that the degradation *in vitro* was similar to that *in vivo* for both materials. Furthermore, scaffold molecular weight had already decreased significantly during the first 4 weeks. In addition, M_n and M_w of the composite scaffold decreased by approximately 90 % during the 24-week follow-up. The neat polymer scaffold had initial M_n and M_w values higher than the composite but the difference in the degradation profile was evened out in 4 weeks, after which no clear differences were seen between the materials or the *in vitro* and *in vivo* environments. The residual L-lactide content after melt-extrusion and scCO₂-foaming for the PLCL scaffold was 0.09 wt% and for the β-TCP/PLCL composite 0.06 wt%.

Viability and proliferation of hASCs *in vitro*

Cell viability was very good since only single dispersed dead cells were observed in cultures. In BM, cell number was clearly less than that in OM at 7 d (Fig. 3) and the difference was evident also at 14 and 21 d. Cell number was similar in OM at 7 d and BM at 21 d.

Cell proliferation was analysed by fluorescent CyQUANT proliferation assay after 7, 14 and 21 d in culture. In concordance with the live/dead staining, cell number was significantly larger in OM in contrast to BM at all time points (Fig. 4a). Moreover, cell number as indicated by live/dead staining was similar in OM at 7 d and BM at 21 d. Variation among the different donor cell lines was evident in proliferation analysis, as OM did not increase the proliferation of hASCs in comparison to BM from one of the donors as it did for the other two.

Osteogenic differentiation of hASCs *in vitro*

ALP activity (Fig. 4b) was significantly greater in OM, in contrast to BM at 7 and 14 d. Furthermore, ALP activity in both BM and OM increased significantly from 7 to 14 d. However, ALP activity did not rise significantly from 14 to 21 d in either BM or OM. ALP activity varied between different donor cell lines and especially one donor cell line had higher ALP activity in comparison to the others.

Total collagen amount did not vary notably among BM and OM groups at 7, 14 or 21 d (Fig. 4c). Collagen amount increased in both study groups slightly from 7 to 14 d; however, collagen amount seemed to decline from 14 to 21 d.

hASCs produced a pronounced mineralised matrix on the composite in both BM and OM at 14 and 21 d (Fig. 4e). Furthermore, they produced notably more mineralised matrix on the scaffold in comparison to hASCs seeded on cell culture plastic (2D) at 21 d (Fig. 4e). At 14 d there was no difference between BM and OM. However, at 21 d, the mineral amount in OM was significantly larger than that in BM (Fig. 4d).

Immunocytochemical staining of COL-I was conducted at 7, 14 and 21 d. In BM, COL-I expression was modest at all time points (Fig. 5a). However, in OM, a clear development of a collagenous matrix was seen during the 3-week experiment: at 7 d, cells were producing COL-I; at 14 d, cells were still producing COL-I and had also excreted COL-I to the extracellular matrix (ECM); at 21 d, there was a strong extracellular COL-I matrix seen in the representative image (Fig. 5a). In addition to COL-I, OCN was also stained at 14 and 21 d. OCN was expressed in both BM and OM at both time points; however, the staining was slightly stronger in OM at both time points (Fig. 5b).

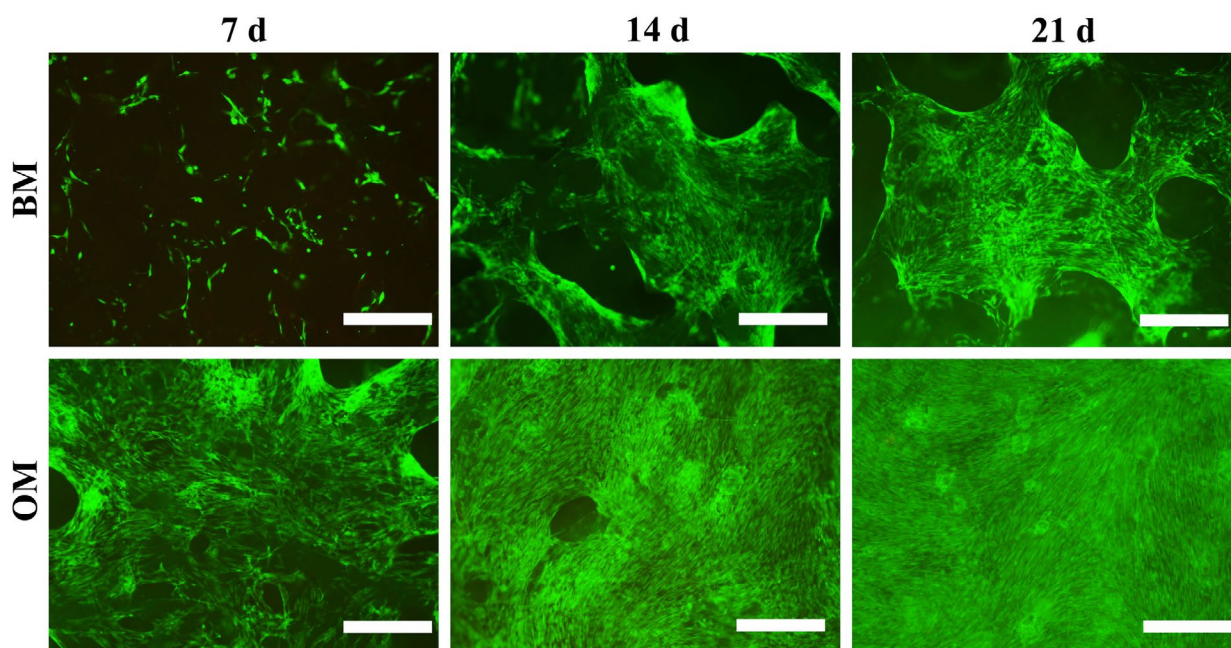


Fig. 3. Viability of hASCs in β-TCP/PLCL composites. Representative images of live/dead stained hASCs cultured in β-TCP/PLCL composites in BM or OM after 7, 14 and 21 d in culture. Scale bar: 500 μm.

qRT-PCR analysis for osteogenic genes *ALP*, *RUNX2a*, *OSX* and *DLX5* was conducted at 7, 14 and 21 d. Relative gene expression did not significantly differ in BM in comparison to OM during the experiment, although, the expression of *RUNX2a* (p values between groups at 7 d: 0.394; 14 d: 0.078; 21 d: 0.310) and *OSTERIX* (p values between groups at 7 d: 0.394; 14 d: 0.123; 21 d: 0.240) was higher in OM as compared to BM at all time points (Fig. 6).

Bone regeneration within composites in rabbit femur defects

Bone was already able to grow on the surface as well as form inside the composite at 4 weeks (Fig. 7). The increased bone growth was observed on the surface and inside the composite at 12 and 24 weeks. In the 4-week μ CT and histological staining images, some

bone formation could be seen beyond the original bone margins, which was most likely a periosteum-induced reaction and not bone formation induced by the implant. Histological staining showed no signs of fibrous tissue or formation of cysts during the 24 weeks. μ CT imaging confirmed the histological staining results. In addition, especially the representative μ CT images at 24 weeks showed that the composite had degraded as compared to 4- and 12-week images (Fig. 7).

Discussion

Composites consisting of calcium phosphates and synthetic polymers have presented promising results in bone engineering applications and it has been

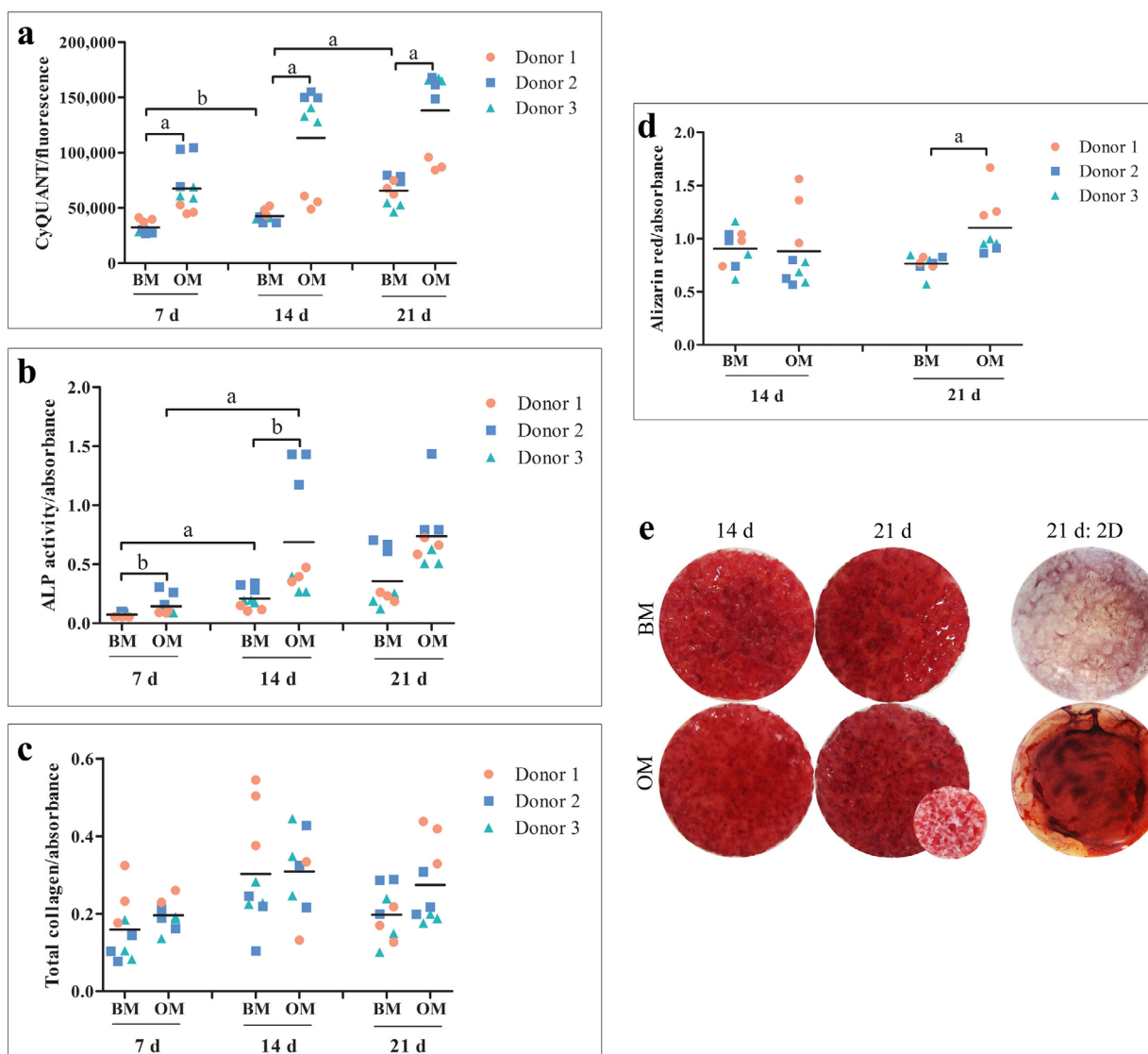


Fig. 4. hASC culture and differentiation in β -TCP/PLCL composites. (a) Cell numbers at 7, 14 and 21 d. (b) ALP activity at 7, 14 and 21 d. (c) Total soluble collagen amount at 7, 14 and 21 d. (d) Quantitative mineralisation results after 14 and 21 d. (e) Representative images of mineral-stained cell-scaffold constructs after 14 and 21 d and of hASC cultures on cell culture plastic (2D) after 21 d. Stained blank scaffold without seeded cells is presented on the left of 21 d OM scaffold (scaffold $\varnothing = 8$ mm; well $\varnothing = 15.5$ mm). Statistical significance indicated as ^a $p \leq 0.001$ or ^b $p < 0.05$ ($n = 9$).

suggested that among biomaterials, composites are the most promising strategy for bone regeneration (de Misquita *et al.*, 2016). scCO₂ processing is a very interesting processing method for polymeric tissue engineering structures as it is totally non-toxic, cost effective and has low critical parameters (T_c : 304 K; P_c : 7.5 MPa) enabling the addition of biomolecules, such as bone morphogenetic protein 2 (BMP-2), into the structure during processing (Duarte *et al.*, 2013). The study aim was to manufacture a composite with high β -TCP content, with porosity similar to that of human cancellous bone. In scCO₂ processing, the higher ceramic content decreases the porosity and

increases the average pore size of the composite (Mathieu *et al.*, 2006). Moreover, 5 wt% β -TCP content has been suggested to be the upper limit in order to obtain a homogenous and interconnected pore structure (Mathieu *et al.*, 2006). In contrast to previous studies, it was possible, for the first time, to create a composite with 50 wt% β -TCP content with porosity as high as 65-67 % and average pore size of 380 μ m by using scCO₂. Previously, Mathieu *et al.* (2006) manufactured polylactide (PLA)/ β -TCP composites by scCO₂ with 74 % porosity but with only 10 % ceramic content. Moreover, Diaz-Gomez *et al.* (2017) reported PCL/fibroin/hydroxyapatite (70/20/10 %)

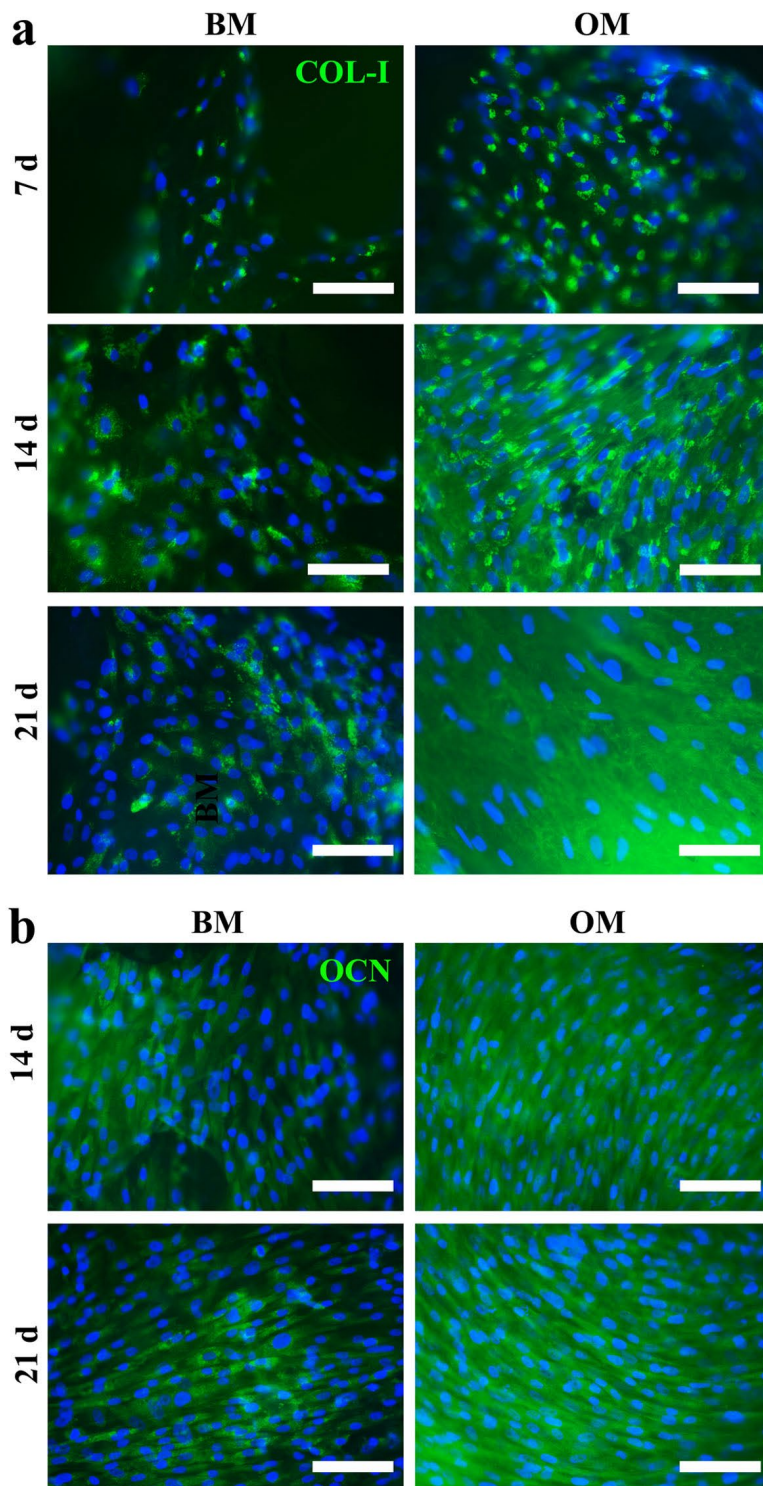


Fig. 5. Immunocytochemical staining of osteogenic markers in hASCs in β -TCP/PLCL composites. Representative images of immunocytochemical staining of (a) COL-I (green) after 7, 14 and 21 d in culture and (b) OCN (green) after 14 and 21 d in culture. Nuclei are stained in blue. Scale bar: 100 μ m.

composites processed by using scCO₂ with average porosity of 69.7 %.

Another challenge related to manufacturing polymer-ceramic composites by using scCO₂ is that the otherwise homogeneously distributed ceramic granules are covered by a polymer surface. To the authors' knowledge, this was the first study overcoming this problem by using a dynamic compression treatment for the composites conducted in an aqueous environment at 37 °C. The treatment tore the polymer surface and β -TCP granules protruded on display as shown in the SEM images. The display of the β -TCP granules on the composite surface is highly important for the early interaction of the composite with cells and tissues, because PLCL lacks biological binding sites (Jeong *et al.*, 2008; Wang *et al.*, 2016) whereas β -TCP has the ability to bind to bone tissue (Barrere *et al.*, 2006; Chatterjea *et al.*, 2013) and induce osteogenic differentiation of mesenchymal stem cells (Marino *et al.*, 2010). In addition, as the compression treatment tore additional holes in the PLCL pore surfaces, it increased the micro porosity and interconnectivity of the composites.

The modulus of the composite was more similar to the modulus of cartilage (2.4-10 MPa) (Beck *et al.*, 2016) than to that of trabecular bone (10.75-13.66 GPa) (Peters *et al.*, 2018), thus mimicking the soft callus formed during natural bone healing. Therefore, a bone defect treated with this composite would still

require additional fixation to restrain the defect site. The closest comparable clinically approved composite material to the study composite is the bone void filler chronOS™ Strip from DePuy Synthes, which comprise PLCL and β -TCP granules. The compression strength of the β -TCP/PLCL composite analysed dry at RT was 1.1 MPa at 20 % strain and 3 MPa at 50 % strain. The compressive strength of the chronOS® β -TCP granules is approximately 5 MPa (product manual of chronOS®), which is of the same order as the strength of the composite described in the current study. However, to the authors' knowledge, the strength of the composite chronOS™ Strip has not been reported. Shikunami *et al.* (2006) compared different P_(D/L)LA-based composites and reported the compression strength of 5.4 MPa for a porous β -TCP/ P_(D/L)LA (weight ratio 70/30) analysed at RT. Moreover, Mathieu *et al.* (2006) reported the compression strength of approximately 3.5 MPa for a porous P_(L)LA/ β -TCP (weight ratio 90/10) composite also analysed dry at RT. As the requirements for an ideal bone substitute are highly demanding, the development of a scaffold may require compromising between achieving good cell and tissue response, desirable mechanical as well as user-friendly properties (Turnbull *et al.*, 2017).

The compression treatment significantly decreased both modulus and strength at 20 and 50 % strain, when samples were tested dry at RT. However, the aqueous

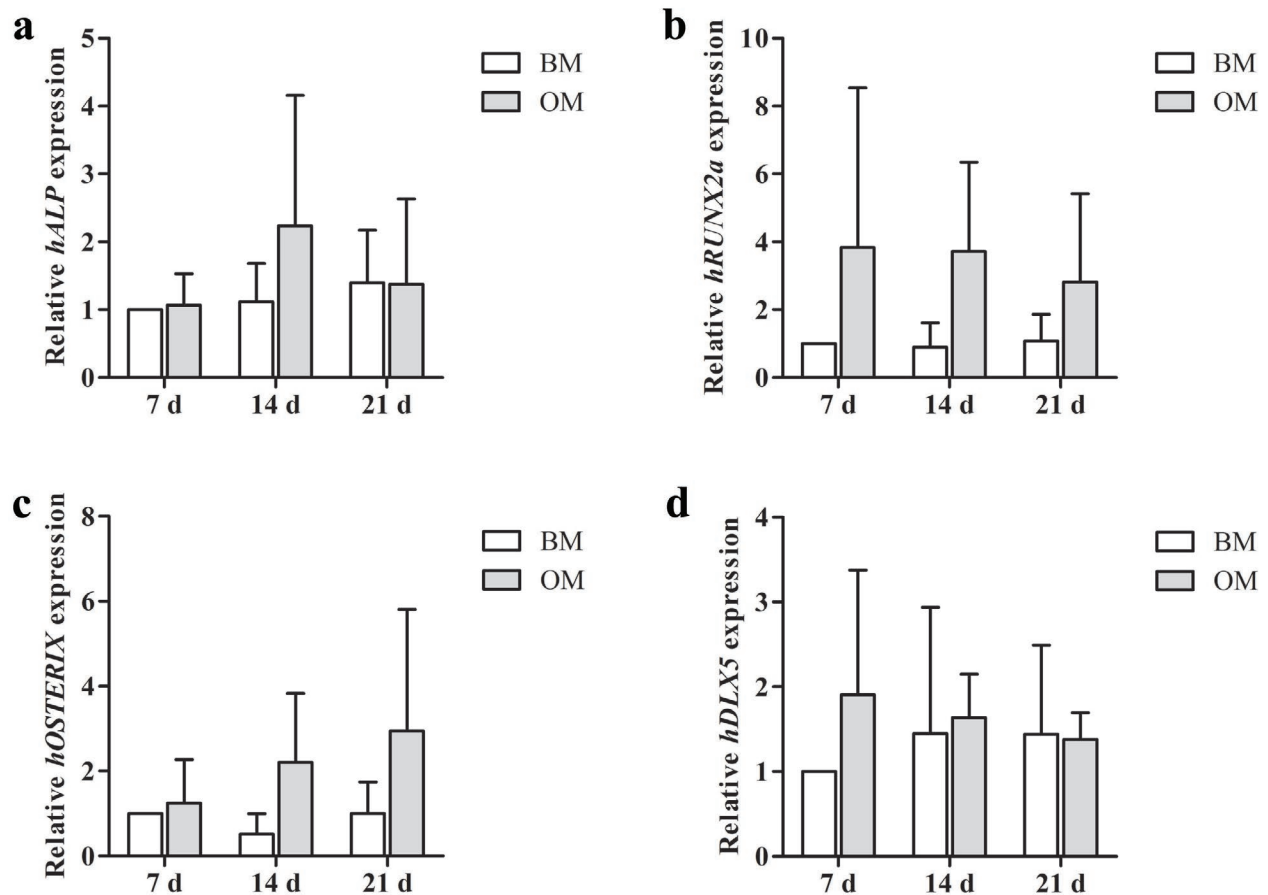


Fig. 6. Relative gene expression of osteogenic genes in hASCs in β -TCP/PLCL composites. (a) ALP, (b) RUNX2a, (c) OSTERIX and (d) DLX5. Results ($n = 6$) are expressed relative to *hRPLP0* and 7 d BM result.

environment at 37 °C, simulating the physiological environment, diminished these differences. This is due to PLCL's glass transition temperature, which is between 21 and 22 °C (Ahola *et al.*, 2013). β -TCP particles were not able to reinforce the porous composite matrix because the polymer chains seemed to be mobile at 37 °C, making the composite highly elastic. During incubation at 37 °C, both intact and pre-compressed composites started to recover from the initial drop of modulus and strength, as there was a rise from 1 h to 7 d at 37 °C. van der Pol *et al.* (2010) proposed that increasing the amount of β -TCP over 5 wt% in a scCO₂-processed composite would make the composite more brittle and make it lose its ability to sustain any deformation. However, present results contradicted this suggestion. The increase in modulus between 1 h and 7 d at 37 °C was likely to be related to the reorganisation of the polymer matrix, *e.g.* crystallisation or an aging type phenomenon in aqueous environment at 37 °C, enabling the polymer chains to organise towards energetically more stable conformations (Pan *et al.*, 2007; Zong *et al.*, 1999). However, within limits of the present study, the true mechanism could not be determined.

By monitoring the hydrolytic degradation both *in vitro* and *in vivo*, the aim was to define how accurately the *in vitro* degradation extrapolated to the situation *in vivo*. Because the degradation characteristics may depend *e.g.* on the polymer or the manufacturing method, the molecular degradation profile *in vitro* may model relatively accurately the degradation *in vivo* (Weir *et al.*, 2004) or differ significantly (Koepp *et al.*, 2004). The results showed that the hydrolytic degradation of the scCO₂-foamed β -TCP/PLCL composite and the following degradation-dependent structural changes could be studied with very good

accuracy in the *in vitro* model. The small differences in the degradation rate during the first 4 weeks could be related to the β -TCP content, which slows down the hydrolytic degradation by neutralising the acidic degradation products of lactide-based polymers (Niemi, 2005). Previously, the same polymer and composite with β -TCP content were studied *in vitro* as non-foamed blocks (Ahola *et al.*, 2013). Despite the different initial molecular weight but similar residual monomer content, the molecular weight was similar after 12 weeks of incubation at 37 °C (Ahola *et al.*, 2013) to that of the present foamed scaffolds.

Results showed that the composites were cytocompatible *in vitro*, as hASC viability was very high, with only some dead cells, as observed by live/dead staining. Both live/dead staining and cell proliferation analysis showed that hASCs proliferated more when cultured in OM as compared to BM, as expected according to previous results with hASCs (Kyllönen *et al.*, 2013a; Tirkkonen *et al.*, 2013; Vanhatupa *et al.*, 2015).

Osteogenic differentiation of hASCs in composites was demonstrated by using various methods. Induction of ALP activity clearly occurred in BM and OM, even though the level of ALP activity was significantly higher in OM than in BM at 7 and 14 d. ALP activity as well as ALP expression peaked at 14 d, as ALP expression is related to the matrix maturation phase of bone ECM development (Lian *et al.*, 2012). Moreover, total soluble collagen amount was generally very similar in both BM and OM. Collagen amount was only slightly larger in OM at 7 and 21 d as compared to BM. The slight decrease in soluble collagen from 14 to 21 d might be due to the development of osteogenic ECM. Mineralised collagen fibrils are the elementary building blocks

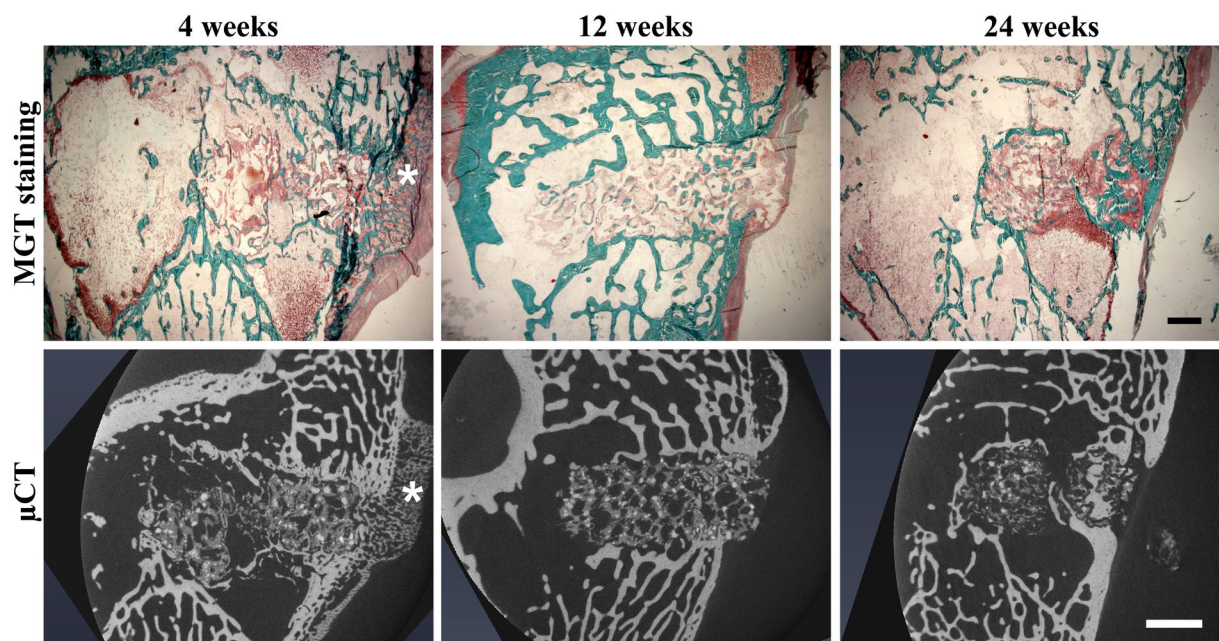


Fig. 7. Bone formation in rabbit femora. Representative images of MGT-stained histological samples (scale bar 1 mm) from rabbit femora with implanted composites and corresponding μ CT imaging (scale bar 2 mm) 4, 12 and 24 weeks after implantation. * indicating periosteum-induced bone formation.

of bone (Nair *et al.*, 2013) and the mineralisation of collagen fibrils may affect the solubility of collagen during soluble collagen analysis. Moreover, dense COL-I matrix promotes the osteogenic differentiation of mesenchymal stem cells attaching to it (Buxton *et al.*, 2008). As alizarin red staining already confirmed the formation of a strong mineralised matrix in both BM and OM at 14 d and the immunocytochemical staining of COL-I was especially strong in OM at 14 and 21 d, it is possible that mineralised collagen matrix, typical of bone development, had developed in cell cultures. In addition, the detection of the late osteogenic marker OCN by immunocytochemical staining confirmed the late osteogenic differentiation of hASCs in the composites (Lian *et al.*, 2012). The expression of osteogenic genes was in line with the literature concerning bone development, as *ALP* and *RUNX2a* expression peaks are related to the early phase of differentiation whereas *OSTERIX* expression peaks to the late phase of differentiation (Lian *et al.*, 2012). Moreover, when comparing the formed mineralised matrix on the scaffold in BM to that on the 2D control in BM, the composite itself seemed to induce osteogenic differentiation of hASCs even without the addition of osteogenic supplements.

Bone regeneration within composites implanted in a rabbit distal femur defect model was demonstrated in a 24-week study. During implantation, the composite proved to be easy to handle and implant due to its elasticity and ability to recover after compression. Poly(L-lactide) implants (Pihlajamäki *et al.*, 2006) and composites (van der Pol *et al.*, 2010) have been shown to induce an inflammatory reaction due to acidic degradation products leading to the development of a fibrous capsule around the implant. However, the femur defect model demonstrated that the biocompatibility of the β -TCP/PLCL composite was good, as no formation of fibrous layer, cysts or infection was detected in any of the animals during the 24-week study. Moreover, the composite was shown to be osteoconductive as, according to the MGT staining and μ CT images, bone was already able to grow on the surface of the composite and infiltrate inside the porous structure at 4 weeks. In contrast to the present results, van der Pol *et al.* (2010) showed that a PLA/ β -TCP (95/5 wt%) composite manufactured by scCO₂ processing induces the formation of a clear fibrous layer between the implant and mineralised tissue at 8 and 16 weeks in sheep femur defects. In concordance with the present results, Pihlman *et al.* (2018) studied the same porous β -TCP/PLCL composites and demonstrated the osteoconductivity and ingrowth of bone and vascular tissue in a rabbit calvarial defect model. Moreover, the β -TCP/PLCL composite gives structural support and blocks the surrounding soft tissues from bulging into the defect (Pihlman *et al.*, 2018). Also, Pihlman *et al.* (2018), in their *in vivo* study, concluded that the mouldable and resilient composite is easier to use in clinics in contrast to most available products used for bone substitutes.

Conclusions

A highly porous, biodegradable, elastic and easy-to-handle β -TCP/PLCL composite to serve as a bone substitute was created. To the authors' knowledge, the present study was the first one reporting a composite manufactured by scCO₂ processing with a high ceramic content (50 wt%) and porosity as high as 65-67 %. Furthermore, β -TCP particles in the processed composites were uncovered by using a dynamic compression treatment.

The β -TCP/PLCL composite was cytocompatible and supported osteogenic differentiation of hASCs *in vitro*. The formation of a collagenous mineralised matrix already after 3 weeks *in vitro* was an especially clear indication of the composite's potential as a bone substitute. Furthermore, the rabbit femur defect model showed that the β -TCP/PLCL composite was biocompatible, as it did not elicit the formation of fibrous capsule, cysts or infection. Finally, the β -TCP/PLCL composite was osteoconductive, as bone tissue was already able to grow on the surface and inside the scaffold at 4 weeks. To conclude, the β -TCP/PLCL composite foamed by using scCO₂ is a very promising bone substitute material and a potential candidate for use in clinics.

Acknowledgements

The work was financially supported by the Finnish Funding Agency for Innovation, a grant from The Finnish Cultural Foundation, Doctoral program of Faculty of Medicine and Life Sciences (University of Tampere) and the Competitive State Research Financing of the Expert Responsibility area of Tampere University Hospital. Authors would like to thank MSc Sanna Karjalainen from Biomaterials and Tissue Engineering Group (BioMediTech, Faculty of Medicine and Health Technology, Tampere University) for her contribution to *in vitro* experiments concerning composite manufacturing and testing and BioCiteHisto Oy (Tampere, Finland) for their expertise in histological samples and stainings. In addition, the authors would like to acknowledge the assistance and excellent equipment of Tampere Imaging Facility (BioMediTech, Faculty of Medicine and Health Technology, Tampere University) and Ms Anna-Maija Honkala, Ms Miia Juntunen and Mrs Sari Kalliokoski for their excellent technical assistance in stem cell isolation and culture.

Authors declare no competing interests.

References

Ahola N, Veiranto M, Rich J, Efimov A, Hannula M, Seppala J, Kellomäki M (2013) Hydrolytic degradation of composites of poly(L-lactide-co-epsilon-caprolactone) 70/30 and beta-tricalcium phosphate. *J Biomater Appl* 28: 529-543.

- Barbour SA, King W (2003) The safe and effective use of allograft tissue – an update. *Am J Sports Med* **31**: 791-797.
- Barrere F, van Blitterswijk CA, de Groot K (2006) Bone regeneration: molecular and cellular interactions with calcium phosphate ceramics. *Int J Nanomedicine* **1**: 317-332.
- Beck EC, Barragan M, Tadros MH, Gehrke SH, Detamore MS (2016) Approaching the compressive modulus of articular cartilage with a decellularized cartilage-based hydrogel. *Acta Biomater* **38**: 94-105.
- Bohner M, Miron RJ (2019) A proposed mechanism for material-induced heterotopic ossification. *Materials Today* **22**: 132-141.
- Boyce T, Edwards J, Scarborough N (1999) Allograft bone. The influence of processing on safety and performance. *Orthop Clin North Am* **30**: 571-581.
- Buxton PG, Bitar M, Gellynck K, Parkar M, Brown RA, Young AM, Knowles JC, Nazhat SN (2008) Dense collagen matrix accelerates osteogenic differentiation and rescues the apoptotic response to MMP inhibition. *Bone* **43**: 377-385.
- Campana V, Milano G, Pagano E, Barba M, Cicione C, Salonna G, Lattanzi W, Logroscino G (2014) Bone substitutes in orthopaedic surgery: from basic science to clinical practice. *J Mater Sci Mater Med* **25**: 2445-2461.
- Chatterjea A, van der Stok J, Danoux CB, Yuan H, Habibovic P, van Blitterswijk CA, Weinans H, de Boer J (2013) Inflammatory response and bone healing capacity of two porous calcium phosphate ceramics in critical size cortical bone defects. *J Biomed Mater Res A* **102**: 1399-1407.
- de Misquita MR, Bentini R, Goncalves F (2016) The performance of bone tissue engineering scaffolds in *in vivo* animal models: a systematic review. *J Biomater Appl* **31**: 625-636.
- Diaz-Gomez L, Garcia-Gonzalez CA, Wang J, Yang F, Aznar-Cervantes S, Cenis JL, Reyes R, Delgado A, Evora C, Concheiro A, Alvarez-Lorenzo C (2017) Biodegradable PCL/fibroin/hydroxyapatite porous scaffolds prepared by supercritical foaming for bone regeneration. *Int J Pharm* **527**: 115-125.
- Dominici M, Le Blanc K, Mueller I, Slaper-Cortenbach I, Marini F, Krause D, Deans R, Keating A, Prockop D, Horwitz E (2006) Minimal criteria for defining multipotent mesenchymal stromal cells. The International Society for Cellular Therapy position statement. *Cytotherapy* **8**: 315-317.
- Doube M, Klosowski MM, Arganda-Carreras I, Cordelieres FP, Dougherty RP, Jackson JS, Schmid B, Hutchinson JR, Shefelbine SJ (2010) BoneJ: free and extensible bone image analysis in ImageJ. *Bone* **47**: 1076-1079.
- Duan R, Barbieri D, de Groot F, de Bruijn JD, Yuan H (2018) Modulating bone regeneration in rabbit condyle defects with three surface-structured tricalcium phosphate ceramics. *ACS Biomater Sci Eng* **4**: 3347-3355.
- Duarte ARC, Santo VE, Alves A, Silva SS, Moreira-Silva J, Silva TH, Marques AP, Sousa RA, Gomes ME, Mano JF (2013) Unleashing the potential of supercritical fluids for polymer processing in tissue engineering and regenerative medicine. *J Supercrit Fluids* **79**: 177-185.
- Freeman FE, McNamara LM (2017) Endochondral priming: a developmental engineering strategy for bone tissue regeneration. *Tissue Eng Part B Rev* **23**: 128-141.
- Holmbom J, Sodergard A, Ekholm E, Martson M, Kuusilehto A, Saukko P, Penttinen R (2005) Long-term evaluation of porous poly(epsilon-caprolactone-co-L-lactide) as a bone-filling material. *J Biomed Mater Res A* **75**: 308-315.
- Jeon O, Rhie JW, Kwon IK, Kim JH, Kim BS, Lee SH (2008) *In vivo* bone formation following transplantation of human adipose-derived stromal cells that are not differentiated osteogenically. *Tissue Eng Part A* **14**: 1285-1294.
- Jeong SI, Lee AY, Lee YM, Shin H (2008) Electrospun gelatin/poly(L-lactide-co-epsilon-caprolactone) nanofibers for mechanically functional tissue-engineering scaffolds. *J Biomater Sci Polym Ed* **19**: 339-357.
- Kinaci A, Neuhaus V, Ring DC (2014) Trends in bone graft use in the United States. *Orthopedics* **37**: e783-788.
- Koepp HE, Schorlemmer S, Kessler S, Brenner RE, Claes L, Günther K, Ignatius AA (2004) Biocompatibility and osseointegration of β -TCP: histomorphological and biomechanical studies in a weight-bearing sheep model. *J Biomed Mater Res B Appl Biomater* **70B**: 209-217.
- Kyllönen L, Haimi S, Mannerström B, Huhtala H, Rajala KM, Skottman H, Sandor GK, Miettinen S (2013a) Effects of different serum conditions on osteogenic differentiation of human adipose stem cells *in vitro*. *Stem Cell Res Ther* **4**: 17. DOI: 10.1186/scrt165.
- Kyllönen L, Haimi S, Säkkinen J, Kuokkanen H, Mannerström B, Sandor GK, Miettinen S (2013b) Exogenously added BMP-6, BMP-7 and VEGF may not enhance the osteogenic differentiation of human adipose stem cells. *Growth Factors* **31**: 141-153.
- Lian JB, Stein GS, van Wijnen AJ, Stein JL, Hassan MQ, Gaur T, Zhang Y (2012) MicroRNA control of bone formation and homeostasis. *Nat Rev Endocrinol* **8**: 212-227.
- Lindroos B, Boucher S, Chase L, Kuokkanen H, Huhtala H, Haataja R, Vemuri M, Suuronen R, Miettinen S (2009) Serum-free, xeno-free culture media maintain the proliferation rate and multipotentiality of adipose stem cells *in vitro*. *Cytotherapy* **11**: 958-972.
- Marino G, Rosso F, Cafiero G, Tortora C, Moraci M, Barbarisi M, Barbarisi A (2010) Beta-tricalcium phosphate 3D scaffold promote alone osteogenic differentiation of human adipose stem cells: *in vitro* study. *J Mater Sci Mater Med* **21**: 353-363.
- Mathieu LM, Montjovent MO, Bourban PE, Pioletti DP, Manson JA (2005) Bioresorbable composites prepared by supercritical fluid foaming. *J Biomed Mater Res A* **75**: 89-97.

Mathieu LM, Mueller TL, Bourban PE, Pioletti DP, Muller R, Manson JA (2006) Architecture and properties of anisotropic polymer composite scaffolds for bone tissue engineering. *Biomaterials* **27**: 905-916.

Nair AK, Gautieri A, Chang SW, Buehler MJ (2013) Molecular mechanics of mineralized collagen fibrils in bone. *Nat Commun* **4**: 1724. DOI: 10.1038/ncomms2720.

Niemelä T (2005) Effect of β -tricalcium phosphate addition on the *in vitro* degradation of self-reinforced poly-L,D-lactide. *Polym Degrad Stab* **89**: 492-500.

Ojansivu M, Vanhatupa S, Björkvik L, Häkkänen H, Kellomäki M, Autio R, Ihalainen JA, Hupa L, Miettinen S (2015) Bioactive glass ions as strong enhancers of osteogenic differentiation in human adipose stem cells. *Acta Biomater* **21**: 190-203.

Pan P, Zhu B, Inoue Y (2007) Enthalpy relaxation and embrittlement of poly(L-lactide) during physical aging. *Macromolecules* **40**: 9664-9671.

Peters AE, Akhtar R, Comerford EJ, Bates KT (2018) The effect of ageing and osteoarthritis on the mechanical properties of cartilage and bone in the human knee joint. *Sci Rep* **8**. DOI: 10.1038/s41598-018-24258-6.

Pihlajamäki H, Böstman O, Tynnenen O, Laitinen O (2006) Long-term tissue response to bioabsorbable poly-L-lactide and metallic screws: an experimental study. *Bone* **39**: 932-937.

Pihlman H, Keranen P, Paakinaho K, Linden J, Hannula M, Manninen IK, Hyttinen J, Manninen M, Laitinen-Vapaavuori O (2018) Novel osteoconductive β -tricalcium phosphate/poly(L-lactide-co- ϵ -caprolactone) scaffold for bone regeneration: a study in a rabbit calvarial defect. *J Mater Sci Mater Med* **29**. DOI: 10.1007/s10856-018-6159-9.

Rouwkema J, Rivron NC, van Blitterswijk CA (2008) Vascularization in tissue engineering. *Trends Biotechnol* **26**: 434-441.

Schindelin J, Arganda-Carreras I, Frise E, Kaynig V, Longair M, Pietzsch T, Preibisch S, Rueden C, Saalfeld S, Schmid B, Tinevez JY, White DJ, Hartenstein V, Eliceiri K, Tomancak P, Cardona A (2012) Fiji: an open-source platform for biological-image analysis. *Nat Methods* **9**: 676-682.

Shikinami Y, Okazaki K, Saito M, Okuno M, Hasegawa S, Tamura J, Fujibayashi S, Nakamura T (2006) Bioactive and bioresorbable cellular cubic-composite scaffolds for use in bone reconstruction. *J R Soc Interface* **3**: 805-821.

Temple JP, Hutton DL, Hung BP, Huri PY, Cook CA, Kondragunta R, Jia X, Grayson WL (2014) Engineering anatomically shaped vascularized bone grafts with hASCs and 3D-printed PCL scaffolds. *J Biomed Mater Res A* **102**: 4317-4325.

Tirkkonen L, Haimi S, Huttunen S, Wolff J, Pirhonen E, Sandor GK, Miettinen S (2013) Osteogenic medium is superior to growth factors in differentiation of human adipose stem cells towards bone-forming cells in 3D culture. *Eur Cell Mater* **25**: 144-158.

Turnbull G, Clarke J, Picard F, Riches P, Jia L, Han F, Li B, Shu W (2017) 3D bioactive composite scaffolds for bone tissue engineering. *Bioact Mater* **3**: 278-314.

van der Pol U, Mathieu L, Zeiter S, Bourban PE, Zambelli PY, Pearce SG, Boure LP, Pioletti DP (2010) Augmentation of bone defect healing using a new biocomposite scaffold: an *in vivo* study in sheep. *Acta Biomater* **6**: 3755-3762.

Van der Stok J, Van Lieshout EM, El-Massoudi Y, Van Kralingen GH, Patka P (2011) Bone substitutes in the Netherlands – a systematic literature review. *Acta Biomater* **7**: 739-750.

Vanhatupa S, Ojansivu M, Autio R, Juntunen M, Miettinen S (2015) Bone morphogenetic protein-2 induces donor-dependent osteogenic and adipogenic differentiation in human adipose stem cells. *Stem Cells Transl Med* **4**: 1391-1402.

Wang Z, Lin M, Xie Q, Sun H, Huang Y, Zhang D, Yu Z, Bi X, Chen J, Wang J, Shi W, Gu P, Fan X (2016) Electrospun silk fibroin/poly(lactide-co- ϵ -caprolactone) nanofibrous scaffolds for bone regeneration. *Int J Nanomedicine* **11**: 1483-1500.

Weir NA, Buchanan FJ, Orr JF, Dickson GR (2004) Degradation of poly-L-lactide. Part 1: *in vitro* and *in vivo* physiological temperature degradation. *Proc Inst Mech Eng H* **218**: 307-319.

Wilson SM, Goldwasser MS, Clark SG, Monaco E, Bionaz M, Hurley WL, Rodriguez-Zas S, Feng L, Dymon Z, Wheeler MB (2012) Adipose-derived mesenchymal stem cells enhance healing of mandibular defects in the ramus of swine. *J Oral Maxillofac Surg* **70**: e193-203.

Yuan H, Fernandes H, Habibovic P, de Boer J, Barradas AM, de Ruiter A, Walsh WR, van Blitterswijk CA, de Bruijn JD (2010) Osteoinductive ceramics as a synthetic alternative to autologous bone grafting. *Proc Natl Acad Sci U S A* **107**: 13614-13619.

Zadpoor AA (2015) Bone tissue regeneration: the role of scaffold geometry. *Biomater Sci* **3**: 231-245.

Zong X, Wang Z, Hsiao BS, Chu B, Zhou JJ, Jamiolkowski DD, Muse E, Dormier E (1999) Structure and morphology changes in absorbable poly(glycolide) and poly(glycolide-co-lactide) during *in vitro* degradation. *Macromolecules* **32**: 8107-8114.

Web Reference

1. <https://eur-lex.europa.eu/legal-content/EN/TXT/?uri=CELEX%3A32017R0745> [05-08-2019]

2. https://worldwide.espacenet.com/publicationDetails/originalDocument?FT=D&date=20190215&DB=&locale=en_EP&CC=FI&NR=127762B&KC=B&ND=4 [12-07-2019]

Discussion with Reviewers

Ryan Porter: Much attention has been paid to the compressive strength of potential bone graft

substitutes. However, existing composite scaffolds with the porosity needed for osteoconduction do not approach the modulus required to replace lost bone function and avoid the need for bone fixation – particularly for lower extremity defects. If immediate restoration of bone mechanical properties is not a design goal, what factors determine the strength needed of candidate scaffolds for bone repair? Would this differ for grafts used in maxillofacial *versus* long bone defects?

Authors: The main aims in composite development are optimal porosity, biocompatibility and osteoconductivity. In addition, easy intra-operative tailoring is highly important, as, for instance, ceramics are not easy to handle or tailor during a surgery, which hinders surgeons' work. With that said, future efforts aim to improve composite mechanical properties to create a composite with similar modulus to subchondral spongiosa. The requirements for mechanical strength of the scaffold are, of course, lower in maxillofacial defects in comparison to long bone defects and, therefore, the composite described in the study is suitable for non-load bearing sites.

Ryan Porter: Supercritical CO₂ has also been used for biomaterial sterilisation processes, including bone allografts. Was the γ-irradiation step included for precautionary measures? Would both steps be required in a good manufacturing practice (GMP) manufacturing protocol for the proposed composite?

Authors: It is true that the processing method can also be used as a sterilisation method. γ-irradiation sterilisation was used for precautionary measures and because it is the commonly used and highly trusted sterilisation method among clinical products. The composite is classified as a medical

device and, therefore, there is no need for a GMP-level manufacturing protocol but an ISO13485 manufacturing protocol is sufficient.

Ryan Porter: What might be the challenges to clinically translate bone graft alternatives manufactured using supercritical CO₂?

Authors: These are highly important matters when developing a clinical product. The challenges in clinical translation of scCO₂-processed structures are related to producing a homogenous pore structure in a reproducible manner. Furthermore, the scalability of the processing is another challenge to overcome in case of a large-scale production.

Pamela Habibovic: A problem of the *in vitro* experiments is the (partially strong) osteogenic differentiation in BM samples. This could indicate pre-differentiation of the used cells, pointing towards an activation of differentiation by the material itself or problems in the assays. This could be clarified by including data of suitable control groups in the results section, *e.g.* cells cultured in BM and OM on tissue culture plastic *etc.*

Authors: The reason for not using a 2D well plate control was the challenge related to the differences between experimental setups in 3D and 2D. Due to these differences, *e.g.* notable differences in cell seeding density and cell attachment, the results between the two setups would not be fully comparable.

Editor's note: The Scientific Editor responsible for this paper was Joost de Bruijn.